Improved Rainfall Measurements from Microwave Link Attenuation Data via MSG SEVIRI Cloud Information

REBECCA WIEGELS[1,2], KATRIN KRZEPEK[1], CHRISTIAN CHWALA[2] & DOROTA IWASZCZUK[1]

Abstract: Adequate spatial coverage of precipitation measurements is not available for large regions. Attenuation data from commercial microwave links (CML) allow precipitation estimates via existing networks, such as the cellular network. However, the processing of the noisy CML data requires a distinction between wet and dry periods. Here, satellite data play a significant role, as they can be used in place of conventional reference data to distinguish between dry periods and precipitation events. In this work, a convolutional neural network is used to process visual and infrared cloud information from geostationary satellites to create a dry indicator. Precipitation products based on satellite data, such as the NWC SAF products PC and PC-Ph, and are utilized as baseline products for comparison. The evaluation shows that the developed Deep Learning (DL) product improves the performance at day- and especially at nighttime. Limitations in detecting the correct rain field area is reduced by the DL product compared to the PC products. In total the DL product improves the Matthews Correlation Coefficient value by about 0.05 compared to the PC-Ph product.

1 Introduction

Reliable and accurate precipitation measurements are crucial for climate observation and for water related issues such as resource management or flood forecasting. However, observation networks have an uneven spatiotemporal global distribution. Data from Commercial Microwave Link (CML), as part of cellular networks, is an additional source for precipitation estimation that has proven to provide valuable rainfall information at a high spatiotemporal resolution (CHWALA & KUNSTMANN 2019). The principal idea is that the signal transmitted from one antenna to the other is attenuated by rainfall, which can then be quantified from the measured attenuation. However, high fluctuations in CML signal levels, which can occur also during dry periods, can hamper the detection of rain events in the recorded data (POLZ et al. 2020). Therefore, several methods exist to separate precipitation from non-precipitation periods such as the widely applied rolling standard deviation approach (SCHLEISS & BERNE 2010) or the 1D Convolutional Neural Network (CNN) approach (POLZ et al. 2020). A detailed listing is given by POLZ et al. (2020). However, the existing methods rely on reference data that do not cover various countries so that a further separation technique is needed which can be applied in precipitation measurement network scarce areas.
Here, satellite data play a significant role, as they can be used in place of conventional reference data to distinguish between dry periods and precipitation events. The satellites remotely sense scattered and emitted radiation from clouds and precipitation. Especially, visual and infrared data of geostationary satellites, which is available in real time, has been used to estimate rainfall

[1] Technical University Darmstadt, Remote Sensing and Image Analysis Department, Franziska-Braun-Str. 7, 64287 Darmstadt, E-Mail: [katrin.krzepek, dorota.iwaszczuk]@tu-darmstadt.de
[2] Institute of Meteorology and Climate Research, KIT, Campus Alpin, Kreuzeckbahnstraße 19, 82467 Garmisch-Partenkirchen, Germany, E-Mail: [rebecca.wiegels, christian.chwala]@kit.edu

(ROEBELING & HOLLEMAN 2009; KIDD & HUFFMAN 2011). The instrument Spinning Enhanced Visible and Infrared Imager (SEVIRI) on board of Meteosat Second Generation (MSG) satellite provides Earth and atmosphere observations at a scale of 15 min and about 3 × 3 km² resolution. SEVIRI observes at 12 spectral channels in the visible and infrared range. The Nowcasting and Very Short Range Forecasting Satellite Application Facility (NWC SAF) developed a wide range of precipitation and cloud products based on SEVIRI data, such as the Precipitation Clouds (PC) and Precipitation Clouds from Cloud Physical Properties (PC-Ph) products. These products, available only for Europe, provide the precipitation probability and have successfully been utilized to improve CML precipitation estimation (VAN HET SCHIP et al. 2017). However, the products have large uncertainties and do not yet exist for the entire area covered by MSG SEVIRI. Therefore, other approaches are needed to improve CML precipitation estimations explicitly in areas where reference data and precipitation cloud products are not available. Other studies have shown that Deep Learning (DL) is capable of predicting cloud properties and precipitation based on MSG SEVIRI satellite data (MORAUX et al. 2019; KIM et al. 2020) and of other geostationary satellites (MA et al. 2022; PFREUNDSCHUH et al. 2022; SADEGHI et al. 2019). Convolutional Neural Networks (CNNs) are specifically designed to recognize visual patterns and process images (GOODFELLOW et al. 2016), which makes satellite imagery a suitable input dataset.
Therefore, this work proposes a CNN approach to yield a dry indicator from MSG satellite data, which is called the DL product throughout this work. Specifically, we aim at developing a wet-dry classification with the future application for CML signal processing to enable precipitation estimation in areas where observation networks are scarce. Thus, the DL product utilizes MSG SEVIRI data as input which, unlike to the PC and PC-Ph products, covers not only Europe but also the African continent. In addition to its potential use throughout the entire MSG SEVIRI covered area, the DL product aims to reduce uncertainties of the precipitation cloud products PC and PC-Ph, such as their limited performance during nighttime. This work evaluates the developed DL product with a direct comparison to the existing baseline products.

2 Data

For this work, native satellite imagery, specifically Level 1.5 SEVIRI data, is used as input for the DL model, while the NWC SAF products PC and PC-PH serve as baseline products. Level 1.5 data is available at EUMETSAT's datastore in HRIT format (EUMETSAT 2022). The precipitation cloud products PC and PC-Ph, produced with software version NWC/GEO v2018, were kindly provided by NWC SAF. The available data includes two months from the 1st of May, 2021 to the 1st of July, 2021 at a 15-minute resolution. The PC product gives the precipitation likelihood from 0 to 100 % with intervals of 10 % for each cloudy pixel. Differently, the PC-Ph product provides the probability of precipitation additionally based on cloud top microphysical properties such as the effective radius, Cloud Optical Thickness and the parallax corrected Cloud Water Path. Note that both final PC and PC-Ph products utilize ancillary data, such as the surface temperature or the geopotential at different pressure levels from Numerical Weather Prediction. (NWC SAF 2019)

As radar reference dataset, the station-corrected radar climatology RADKLIM-YW of the German Weather Service (DWD), which provides 5-minute precipitation rates, is applied. The data is available with an equidistant grid of 1 km² spatial resolution, covering Germany with 1100 × 900 grid cells.

3 Methods

As DL model, a Convolutional Neural Network (CNN) was chosen to conduct the wet-dry classification. For this purpose, the model was fed with several channels of MSG SEVIRI, and trained with the radar reference set. The dataset of the full time period is split into three subsets. One is used to train the model, one is used for validation and optimization and the third subset is used for testing and remains unseen during training and optimization. The test subset consists of 584 samples, a 6-day period, of which each covers the full domain of the radar reference with 180 × 252 grid cells. Differently, the training and validation samples consist of small patches, of which each patch covers an area of roughly 50 × 27 km² with 9 × 9 grid cells.

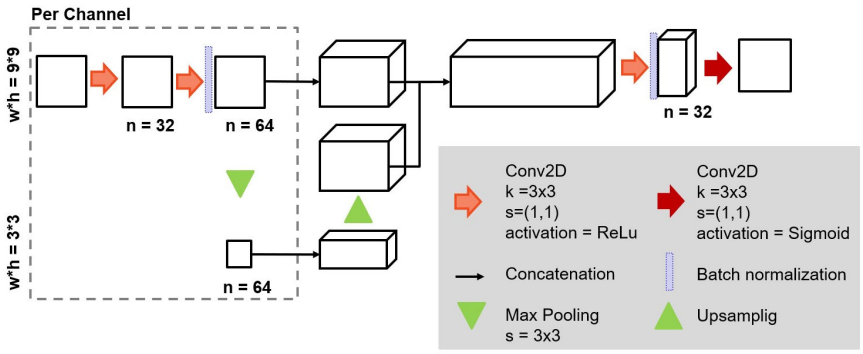

Fig. 1: A graphical illustration of the CNN architecture. The section within the dashed box indicates that the layers are applied per channel individually and then concatenated as indicated

The architecture of the proposed CNN model is shown in Figure 1. The details of the number of kernels (n), kernel size (k), stride (s) and activation function type are given in the figure. Each input sample consists of a set of channels, two infrared (IR 3.9 & IR 10.8), one water vapor (WV 6.2) and one visible channel (VIS 0.6). The input is preprocessed with a separated min-max normalization applied to all channels of one unit. They are separately convolved (SADEGHI et al. 2019) and downsampled by a max-pooling layer in order to maintain and learn information of each channel individually. The previous layers are kept to transfer pre-max pooling information, as done by MORAUX et al. (2019), to recover the high-resolution information which is lost during max-pooling. The downscaled concatenated feature maps are then upsampled with a transposed convolutional layer. The final feature maps are derived by applying a last convolutional layer. The ability to generalize is encouraged by utilizing batch normalization. Finally, the network outputs a continuous wet probability in a range of [0, 1] at the same temporal and spatial resolution as the input. This leads to a total of 233,441 trainable parameters. Since, the dataset is made up of around 90% dry and only 10% wet pixels, an imbalanced dataset is at hand. To balance the dataset, not all patches that are composed of only dry pixels are considered for training. The optimized settings

for model and input dataset were estimated through hyper-parameter tuning. This resulted in a learning rate of 10^{-4}, batch size of 128, the binary cross-entropy as loss function and a 10 % share of patches exclusively consisting of dry pixels.

Table 1: Binary measures, their output ranges and optimum

Measure	Formula	Range	Optimum
True Positive Rate	TP / (TP+FN)	[0,1]	1
True Negative Rate	TN / (TN+FP)	[0,1]	1
False Negative Rate	FN / (TP+FN)	[0,1]	0
False Positive Rate	FP / (TN+FP)	[0,1]	0
Overall Accuracy	(TP+TN) / (FP+FN)	[0,1]	1
MCC	$\frac{\mathrm{TP}\cdot\mathrm{TN} - \mathrm{FN}\cdot\mathrm{FP}}{\sqrt{(TP+FP)(TP+FN)(TN+FP)(TN+FN)}}$	[-1,1]	1

For the evaluation, a binary mask is applied to the probabilistic output to generate the needed dry-wet classification. Then, binary classification scores (Table 1) can be applied. The confusion matrix helps to sort classification results into four classes. Correctly classified samples are referred to as True Positives (TP) and True Negatives (TN). The error types are grouped into False Positives (FP) and False Negatives (FN). The normalized measures include True Positive Rate (TPR), False Positive Rate (FPR), True Negative Rate (TNR) and True Negative Rate (TNR). Additionally, to address all parameter the Overall Accuracy (OA) and the Matthews Correlation Coefficient (MCC) are applied, of which the latter is less sensitive to class balance.
The Receiving Operating Characteristic (ROC) is utilized additionally, where TPR is plotted over FPR. The ROC curve visualizes the trade-off of threshold choice, thus, the benefits of high TP numbers and costs of high FP numbers, which is especially relevant for rain event detection approaches. Generally, the point (0,1) represents a perfect classifier. Contrarily, random guessing is represented by the diagonal [(0,0), (1,1)].

4 Results & Discussion

The overall performance is evaluated with the help of the above described measures. Table 2 lists the scores of the DL product as well as both baseline products. Note, the threshold for each product is chosen based on which produced the highest MCC score. The DL product outperforms both baseline products in terms of OA, MCC and FPR. However, the TPR is the highest for the PC Product with a rate of 0.79 compared to 0.65 of DL Product. This is due to the fact, that the baseline products score the highest MCC for a low threshold which in turn means that the wet predictions increase. Thus, the baseline product performs well in detecting precipitation but in turn gives up a high number of correct true dry predictions (TN).
Related studies that apply CNN to yield precipitation based on satellite data perform similar or higher in terms of TPR. SADEGHI et al. (2019) estimated the hourly precipitation intensities based

on infrared and water vapor geostationary satellite observations in the USA. Similarly, MORAUX et al. (2019) developed a CNN to generate precipitation intensities over Europe, however, utilizing MSG SEVIRI and rain gauge data as input data. Both studies included categorical scores in their evaluation allowing a direct comparison to the DL product. The DL product scored in overall 0.65, which is within the magnitude of PERSIANN-CNN (SADEGHI et al. 2019) with TPR 0.67, which. The CNN model of MORAUX et al. (2019) with 15-minute resolution estimation scored a TPR of 0.47 and FPR of 0.08. Yet, the authors reveal higher scores for combined DL predictions based on MSG SEVIRI and additionally rain gauge and topography data.

Table 2: Overall performance of DL prediction (threshold at 0.5) and the baseline products (threshold ad 10%). Bold values indicate the scores closest to the optimum for each measure

	OA	MCC	TPR	FPR	TP [$\cdot 10^6$]	FP [$\cdot 10^6$]	FN [$\cdot 10^6$]	TN [$\cdot 10^6$]
DL product	**0.93**	**0.55**	0.65	**0.05**	0.76	**0.65**	0.42	**12.84**
PC-Ph	0.89	0.50	0.71	0.09	0.97	1.24	0.4	12.07
PC	0.85	0.47	**0.79**	0.14	**1.07**	1.85	**0.29**	11.46

The choice of threshold influences the scores of binary inputs strongly. Therefore, the ROC curve is used as an additional measure to assess the performance. Fig. 2 reveals the high performance of the DL product at any chosen threshold. At any point, the ROC curve of the DL product (red points) is closer to the point (0,1), which is the point that indicates a perfect classifier, than the ROC curve of the PC-Ph product.

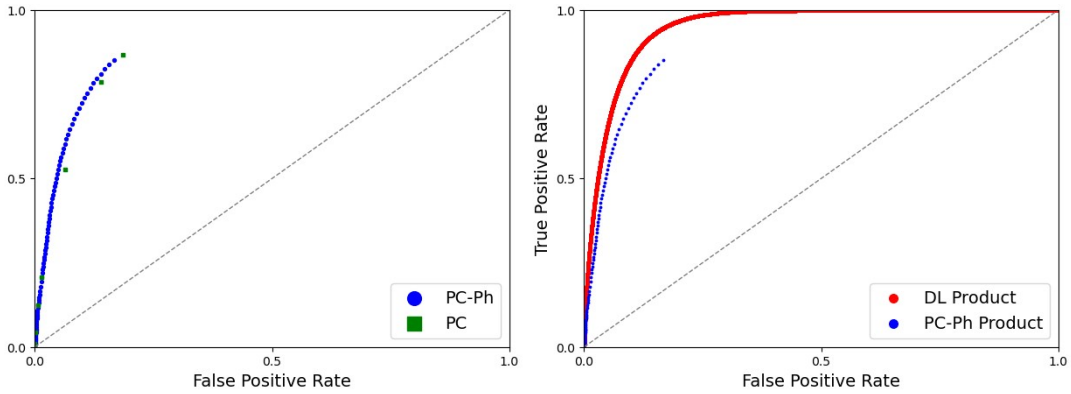

Fig. 2: The ROC curves of the DL product compared to the PC-Ph product in blue (left) and both baseline product compare to each other on the right

The baseline products and other studies (KUMAH et al. 2021) show a performance drop during night compared to daytime. Fig. 3 highlights this decrease of performance as the differences between filled and striped bars, representing the MCC scores calculated for images during day and night. The mean drop of MCC between day and night is reduced by the DL product from 0.26 of PC and 0.10 of PC-Ph to 0.06. Moreover, the DL product scores a higher MCC at both day and night. During daytime the highest MCC score of the baseline products reaches 0.59 and the DL

product reaches 0.60. At night the difference of highest MCC between baseline and DL product is increased with a difference of 0.12.

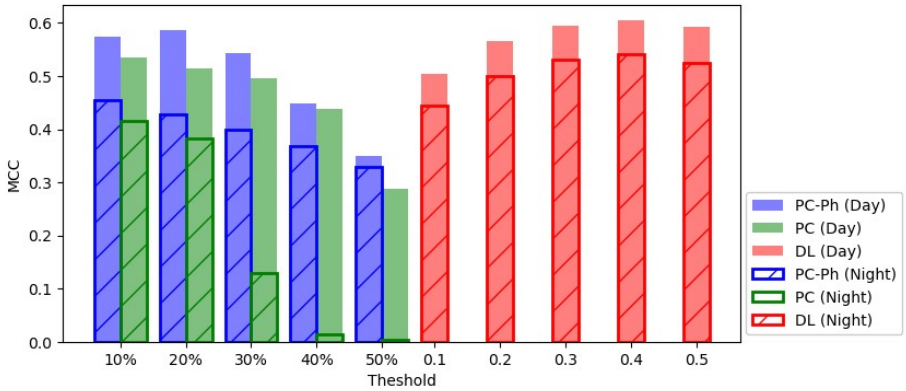

Fig. 3: The MCC score of the DL, PC and PC-Ph products, but distinguished between daytime (filled bars) and night-time (striped bars in front), plotted for different threshold choices

The evaluation between day and night indicates a particular improvement during night-time. Therefore, qualitative visualizations of night- (a), (b) and daytime (c) are shown in Fig. 4. All sub-figures show a reduction of FPs (false positive, i.e. falsely classified as wet) in purple for the DL product. Nevertheless, the DL product is able to correctly classify the dry classified pixels (grey) in an example when no precipitation occurred in Germany, where the PC products generate FPs (b). However, these visualizations show that all three products have limitations in capturing the exact outline of a rainfall field and in correctly classifying small individual patches of rainfall. The issue of correctly classifying wet and dry pixels for the later case can be found in the centre of Fig. 4(c), where both error types, FPs in purple and FNs in orange, occur for all three products.
This work's limitations lie within the temporal scope and regional dependency of the developed DL product. Firstly, the overarching objective of this work is to apply the DL method and product to other regions where radar data is not available. The DL product trained with German target data, will most likely show a decreased performance in regions with different climatic conditions and therefore unseen cloud and precipitation relations. Secondly, MORAUX et al. (2019) point out that the main difficulty of a satellite DL approach is to distinguish clouds with a low precipitation rate of non-precipitation clouds, which occur more frequently in winter of the northern hemisphere. Therefore, the DL product is expected to show a decreased performance during winter time and explains the especially good performance for a short period of time in Germany's summer time.

5 Conclusions

In this study, the applicability of a CNN (DL product) to detect dry and wet areas based on MSG SEVIRI information was demonstrated for day- and night-time in the study area of Germany at a 6-day summer period. Compared to the existing baseline products PC and PC-Ph from NWC SAF, the DL product shows clear improvements of the MCC, which is most prominent during night-time. However, the baseline products, when choosing the threshold for highest MCC, perform better in terms of the TPR and FNR.

Altogether, based on the findings of this work, it can be concluded that a DL approach to create a dry indicator of satellite data is a promising method. However, since the overall goal is that the dry indicator can be applied to improve CML precipitation estimations in future, especially in areas where only sparse precipitation networks exist, it is suggested that the promising DL results are evaluated for different regions and seasons. In this work, the evaluation time period is limited to 6 days of June 2022. Therefore, further studies require to test the promising results for a longer time period, especially for a time period that includes seasonal differences.

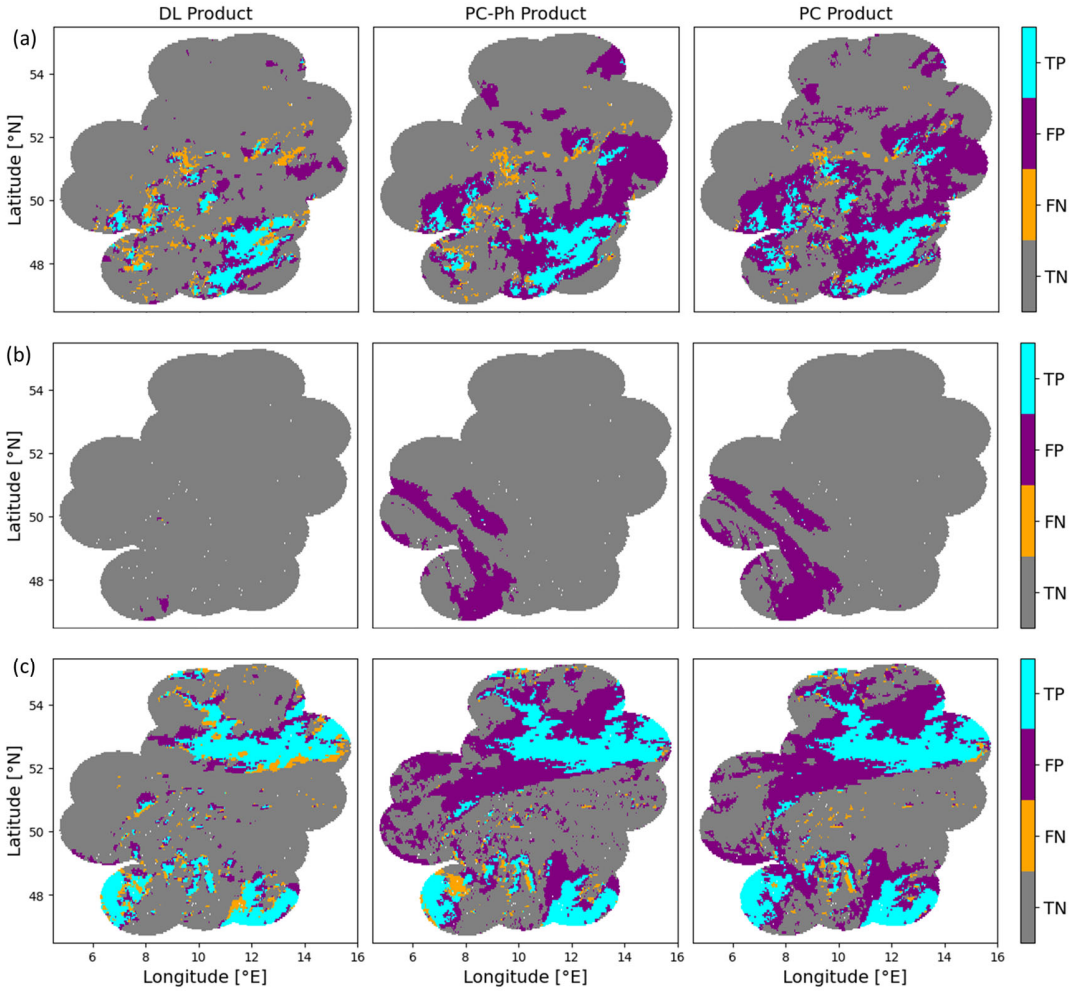

Fig. 4: Qualitative differences shown between DL, PC and PC-Ph products in correctly detecting rainfall (cyan), correctly detecting dry pixels (grey) and false predictions for rainfall (purple) and dry pixels (orange). From (a) to (c) the dates of these examples are 2022-06-25 00:30, 2022-06-27 02:30 and 2022-06-30 13:15

6 Code Availability

The code used for the processing of data and of the DL model developed for this work can be found in the published repository (WIEGELS et al. 2024).

7 References

CHWALA, C. & KUNSTMANN, H., 2019: Commercial microwave link networks for rainfall observation: Assessment of the current status and future challenges. Wiley Interdisciplinary Reviews: Water, **6**(2), https://doi.org/10.1002/WAT2.1337.66.

GOODFELLOW, I., BENGIO, Y. & COURVILLE, A., 2016: Deep Learning. MIT Press. http://www.deeplearningbook.org, last access 03.02.24.

KIDD, C. & HUFFMAN, G., 2011: Global Precipitation measurement. Meteorological Applications, 334-353.

KIM, M., CERMAK, J., ANDERSEN, H., FUCHS, J. & STIRNBERG, R., 2020: A New Satellite-Based Retrieval of Low-Cloud Liquid-Water Path Using Machine Learning and Meteosat SEVIRI Data. Remote Sensing, **12**(21), 1-16.

EUMETSAT, 2022: Earth Observation Portal. https://eoportal.eumetsat.int/, last access 03.02.24.

KUMAH, K.K., MAATHUIS, B. H. P., HOEDJES, J. C. B., RWASOKA, D. T., RETSIOS, B. V. & SU, B. Z., 2021: Rain Area Detection in South-Western Kenya by Using Multispectral Satellite Data from Meteosat Second Generation. Sensors, **21**, 3547.

MA, Z., ZHU, S. & YANG, J., 2022: FY4QPE-MSA: An All-Day Near-Real-Time Quantitative Precipitation Estimation Framework Based on Multispectral Analysis from AGRI Onboard Chinese FY-4 Series Satellites. IEEE Transactions on Geoscience & Remote Sensing, **60**, 1-15.

MORAUX, A., DEWITTE, S., CORNELIS, B. & MUNTEANU, A., 2019: Deep learning for precipitation estimation from satellite and rain gauges measurements. Remote Sensing, **11**(21).

NWC SAF, 2019: Algorithm Theoretical Basis Document for the Precipitation Product Processors of NWC/GEO. NWC/CDOP2/GEO/AEMET/SCI/ATBD/Precipitation Issue 2.1.

PFREUNDSCHUH, S., INGEMARSSON, I., ERIKSSON, P., VILA, D. A. & CALHEIROS, A. J. P., 2022: An improved near-real-time precipitation retrieval for Brazil. Atmos. Meas. Tech., **15**, 6907-6933, https://doi.org/10.5194/amt-15-6907-2022.

POLZ, J., CHWALA, C., GRAF, M. & KUNSTMANN, H., 2020: Rain event detection in commercial microwave link attenuation data using convolutional neural networks. Atmospheric Measurement Techniques, **13**(7), 3835-3853.

ROEBELING, R.A. & HOLLEMAN, I., 2009: SEVIRI rainfall retrieval and validation using weather radar observations. Journal of Geophysical Research Atmospheres, **114**(21).

SADEGHI, M., ASANJAN, A.A., FARIDZAD, M., NGUYEN, P., HSU, K., SOROOSHIAN, S. & BRAITHWAITE, D., 2019: PERSIANN-CNN: Precipitation estimation from remotely sensed information using artificial neural networks–convolutional neural networks. Journal of Hydrometeorology, **20**(12), 2273-2289.

SCHLEISS, M. & BERNE, A., 2010: Identification of dry and rainy periods using telecommunication microwave links. IEEE Geoscience and Remote Sensing, https://doi.org/10.1109/LGRS.2010.2043052.

VAN HET SCHIP, T. I., OVEREEM, A., LEIJNSE, H., UIJLENHOET, R., MEIRINK, J. F. & VAN DELDEN, A. J., 2017: Rainfall measurement using cell phone links: classification of wet and dry periods using geostationary satellites, Hydrological Sciences Journal, **62**(9), 1343-1353.

WIEGELS, R., GLAWION, L., POLZ, J. & CHWALA, C., 2024: MSG SEVIRI CNN wet-dry code package. https://github.com/RebWiegels/MSG-SEVIRI-CNN-wet-dry, last access 08.01.24.